American Journal of Transplantation 2015; 15: 1682–1691
Wiley Periodicals Inc.

doi: 10.1111/ajt.13161

Brief Communication

MicroRNA-494 Promotes Cyclosporine-Induced Nephrotoxicity and Epithelial to Mesenchymal Transition by Inhibiting PTEN

J. Yuan[1], C. J. Benway[1,2], J. Bagley[1] and J. Iacomini[1,2,*]

[1]*Department of Developmental, Molecular and Chemical Biology, Tufts University School of Medicine, Boston, MA*
[2]*Sackler School of Biomedical Sciences Programs in Immunology and Genetics, Boston, MA*
[*]*Corresponding author: John Iacomini, john.iacomini@tufts.edu*

A major complication associated with cyclosporine (CsA) treatment is nephrotoxicity. In this study, we examined whether microRNAs play a role in cyclosporine-induced nephrotoxicity. Treatment of mice with CsA resulted in nephrotoxicity that was associated with an early increase in expression of microRNA mmu-miR-494 (miR-494). Similarly, tubular epithelial cell epithelial-mesenchymal transition (EMT) induced by CsA toxicity resulted in the upregulation of microRNA-494 and a decrease in PTEN levels in vitro. miR-494 directly targeted *Pten* and negatively regulated its expression. Preventing *Pten* targeting by miR-494 was sufficient to prevent CsA induced EMT. Knockdown of miR-494 prevented the downregulation of PTEN in tubular epithelial cells following CsA treatment and also prevented CsA induced EMT. Thus, miR-494 plays a major role in promoting CsA induced nephrotoxicity through its ability to target *Pten* thereby contributing to EMT. We suggest that manipulating miR-494 expression may represent a novel approach to preventing EMT associated with CsA induced nephrotoxicity.

Abbreviations: a-SMA, α-smooth muscle actin; b-gal, b-galactosidase; CCN, chronic cyclosporine nephrotoxicity; CsA, cyclosporine A; EMT, epithelial to mesenchymal transition; FSP-1, fibroblast specific protein-1; GAPDH, Glyceraldehyde 3-phosphate dehydrogenase; LNA, locked nucleic acid; miR, microRNA; PAS, periodic acid Schiff; PCR, polymerase chain reaction; PTEN, phosphatase and tension homolog; SDS-PAGE, sodium dodecyl sulfate polyacrylamide gel electrophoresis; TEC, tubular epithelial cell; UTR, untranslated region; UUO, unilateral ureteral obstruction

Received 08 December 2014, and accepted for publication 11 December 2014

Introduction

The use of cyclosporine A (CsA) has led to dramatically reduced acute rejection of solid organ transplants through its ability to prevent T cell activation (1). The ability of CsA to suppress T cell-mediated immune responses has also led to its application in the treatment of autoimmune diseases (2,3). However, short- or long-term use of CsA is associated with nephrotoxicity in renal transplant and non-transplant patients (1,4,5). Acute CsA nephrotoxicity is reversible following CsA withdrawal while chronic CsA nephrotoxicity (CCN) is irreversible. The mechanisms leading to CCN are not fully understood, although injury appears to result from processes that lead to apoptosis of renal tubular cells, the generation of reactive oxygen species, and epithelial-mesenchymal transition (EMT) that causes fibrosis (6–9).

MicroRNAs (miRs) are small noncoding RNAs that regulate gene expression posttranscriptionally. Changes in miR expression resulting in altered expression of their mRNA targets has been implicated in the pathogenesis of a growing number of disease processes and clearly exerts a functional role in the kidney (10). Here we examined whether miRs play a role in regulating CsA nephrotoxicity. Together, our data suggest that the upregulation of miR-494 is an early event associated with tubular epithelial injury, and contributes to EMT induced through inhibition of PTEN.

Materials and Methods

Animals

Ten- to twelve-week-old male C57BL/6J mice were purchased from The Jackson Laboratory (Bar Harbor, ME) and housed under microisolator conditions. All experiments were performed in accordance with the humane use and care policies of our Institution and were approved by the standing IACUC.

Induction of CsA nephrotoxicity in vivo

CsA nephrotoxicity was induced as in (11,12). Briefly, mice were placed on a low sodium diet (0.01% sodium, TD.90228, Harlan laboratories, USA) and received a daily subcutaneous injection of CsA diluted in olive oil (MP Biomedicals, Solon, OH). Control mice (vehicle) received a daily subcutaneous injection of olive oil only. Each group included 4–5 animals.

Unilateral ureteral obstruction (UUO)

Unilateral obstruction was induced by ligating the left ureter as in (13). The right kidney served as control.

Cell culture

HK-2 cells were cultured in serum-free keratinocyte medium (Gibco, USA) and maintained at 37°C in a humidified atmosphere containing 95% air and 5% CO_2. CsA was prepared as a stock solution (5 μg/μL) in 100% ethanol. 80–90% confluent HK-2 cells were treated with CsA at predetermined concentrations or ethanol (0.1%, as vehicle control).

Histology

Kidneys were harvested, fixed in 10% buffered formalin and Periodic acid-Schiff (PAS) staining was performed. Tubular injury and arteriolopathy were evaluated as previously described (11).

Immunocytochemistry

HK-2 cells were cultured on collagen-coated coverslips, fixed in 10% buffered formalin, and permeabilized with Triton-100 in PBS. After blocking with 2% goat serum in PBS, cells were incubated with anti-α-SMA, or FSP-1 antibody. Subsequently, the cells were incubated with DyLight488 conjugated goat anti-mouse IgG2a antibody (1:200, Biolegend, San Diego, CA). Images were captured using a SPOT RT3 CCD camera (SPOT Imaging Solutions, Sterling Heights, MI) mounted to a Nikon TE300 Nikon microscope system.

Western blot

Kidney and cell lysates were separated by conventional SDS-PAGE and subjected to Western blot analysis using standard methods. Antibodies used were as follows: PTEN (Cell Signaling Technology, Cambridge, MA), E-cadherin (BD biosciences, San Jose, CA), α-SMA (Sigma–Aldrich, St. Louis, MO), and GAPDH (Sigma–Aldrich, St. Louis, MO). Western blots were quantified using Image Lab version 5.0 (Bio-Rad, Hercules, CA).

Real time quantitative PCR

Total RNA extraction and real time PCR were performed as in (14). All data were acquired using a Bio-Rad CFX96 real time PCR system and analyzed using CFX Manager Software v3.1 (Bio-Rad). Relative quantification was calculated using the ΔΔCT method.

Pten *expression studies*

A cDNA encoding murine *Pten* lacking the 3′UTR containing miR-494 targeting sequences was cloned into the MIGR1 expression vector (PTEN-MIGR1, a kind gift of Lawrence A. Turka, Massachusetts General Hospital, Boston, MA). PTEN-MIGR1 was then transfected into HK-2 cells. After 24 h, 5 μg/mL CsA or vehicle was added into the medium for 48 h. Control cultures were transfected with an empty MIGR1 vector.

Luciferase assays

The 3′UTR of murine *Pten* was amplified by PCR and cloned down-stream of the luciferase reported gene in pMIR-REPORT (Ambion-Life Technologies, Grand Island, NY). Cells were transfected with the luciferase reporter and a control vector expressing β-gal using FuGENE HD (Promega, Madison, WI). After 24 h, a miR-494 mimic (30 nM) or scrambled miR mimic negative control (Ambion) was added into the medium for 48 h. Cells were lysed and luciferase activity determined using the Dual-Luciferase Reporter Assay System (Promega) according to the manufacturer's instructions. All data were acquired using a GloMAx-Multi + microplate instrument (Promega).

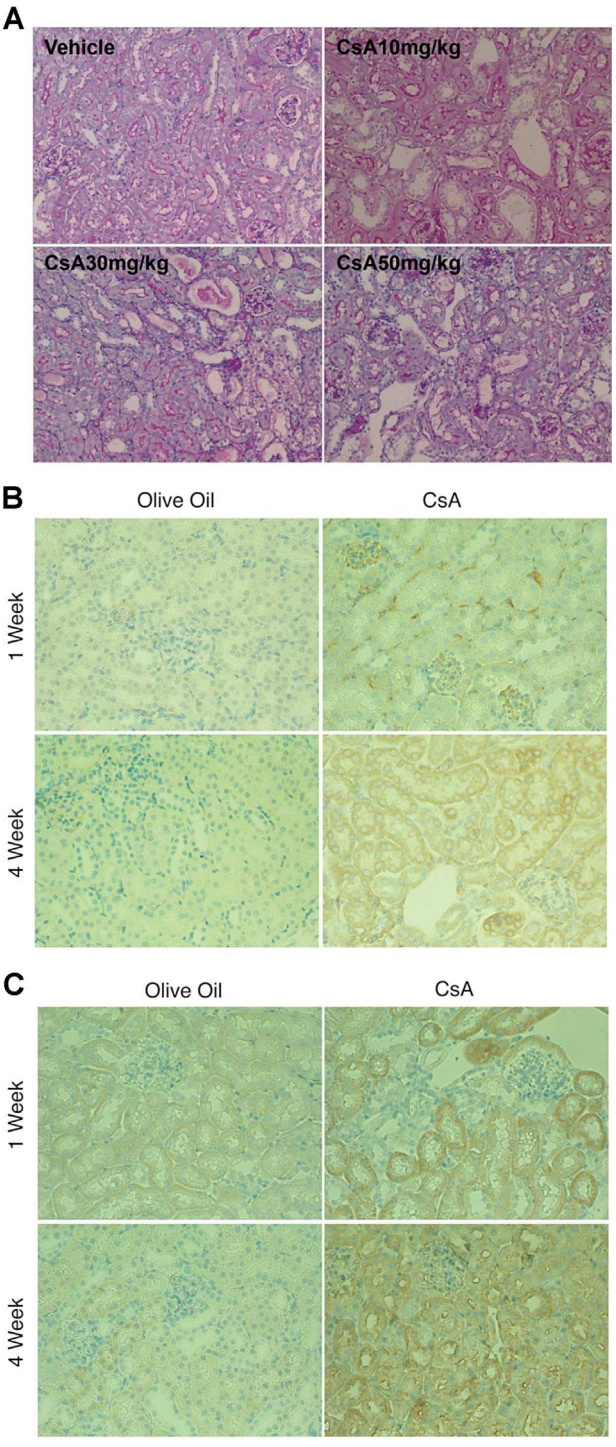

Figure 1: C57BL/6J mice were treated with CsA for 4 weeks and renal injury was assessed. (A) Periodic acid-Schiff stained kidney tissue sections from mice treated with various doses of CsA or vehicle. (B) Staining of kidney tissue sections from mice treated with CsA or vehicle for α-SMA. (C) Staining of kidney tissue sections from mice treated with CsA or vehicle for FSP-1. Shown are representative tissue sections. All magnifications are shown at 200×.

miR-494 knockdown

Locked-nucleic acid (LNA) antagomirs specific for miR-494 as well as scrambled control antagomirs were purchased from Exiqon (Woburn, MA) and transfected into HK-2 cells using Lipofectamine RNAiMAX reagent according to the manufacturer's instructions (Life Sciences, Grand Island, NY).

Statistical analysis

Data were analyzed by unpaired Student's t-test or one-way ANOVA. A value of $p < 0.05$ was considered statistically significant. ** indicates p values of <0.005. * indicates p values of <0.05.

Results

Induction of renal damage in mice treated with CsA

To examine the role of miRs in CsA induced nephrotoxicity, C57BL/6J mice were treated with 10, 30, or 50 mg/kg/day of CsA for 4 weeks. All mice were maintained on a low salt diet to increase their sensitivity to CsA induced damage as described previously (11). After 4 weeks, mice were sacrificed and kidneys harvested to assess damage. Histological analysis revealed that kidneys from mice in all groups exhibited tissue damage the severity of which correlated with the dose of CsA administered (Figure 1A). Kidneys from all groups exhibited arteriopathy and tubular injury as expected (Figure S1A and B). Mice receiving 30 or 50 mg/kg/day CsA also exhibited an increase in serum creatinine (Figure S1C). Kidneys from mice receiving 30 or 50mg/kg/day CsA also showed an increase in expression of α-smooth muscle actin (α-SMA), and fibroblast specific protein-1 (FSP-1) but not E-cadherin (Figure 1B and C and Figure S1E and F) indicating fibrosis (8,15–17). Mice receiving 50 mg/kg/day CsA often exhibited signs of infection, presumably as a result of CsA mediated immunosuppression. Because treatment with 30 mg/kg/day CsA resulted in an increase in serum creatinine but was not associated with infections, we used this dose for the majority of our *in vivo* studies.

CsA nephrotoxicity results in alterations in miR-494 expression

We next sought to identify miRs that might be involved in regulating genes that contribute to CsA nephrotoxicity. Initial studies using microRNA expression profiling

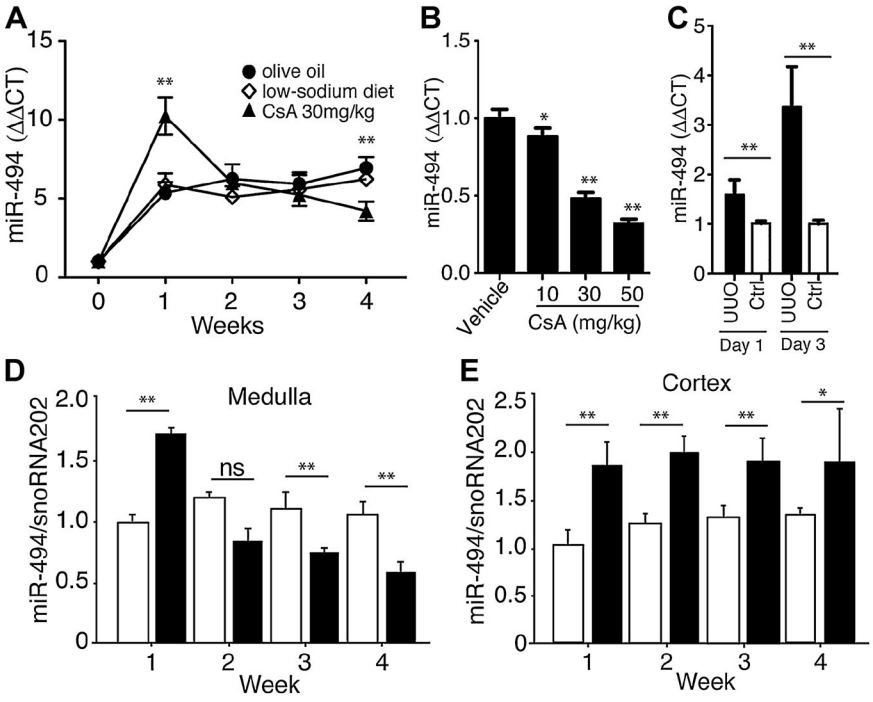

Figure 2: (A) Expression of miR-494 in the kidneys of treated mice. All mice were placed on a low sodium diet and received no further treatment (low sodium diet, open diamonds), olive oil (vehicle, closed circles), or 30 mg/kg CsA dissolved in olive oil (CsA 30 mg/kg, triangles). The volume of olive oil given was the same as the volume CsA given. Mice were sacrificed after 1, 2, 3, and 4 weeks of treatment and kidneys harvested. Untreated mice were used as controls for the 0 week time point. Data are representative of two independent experiments (n = 5 mice per group). (B) Analysis of miR-494 expression in the kidneys of mice treated with vehicle or 10, 30, or 50 mg/kg/day CsA for 4 weeks. (C) Expression of miR-494 in the kidneys on day 1 or 3 post-UUO. Data are representative of at least two independent experiments (n = 4–5 mice per group). Expression of miR-494 in the medulla (D) and cortex (E) of mice treated with CsA (solid bars) or vehicle (open bars). miR-494 expression was quantitated as above (n = 4 mice per group). In all cases, expression of miR-494 was assessed by real-time PCR and expressed as ΔΔCT following normalization to snoRNA202. Bars and data points represent means ± SEM.

indicated that expression of miR-494 is altered in samples prepared from the kidneys of C57BL/6 mice treated with CsA when compared with control kidneys over time (Figure 2A). After one week, expression of miR-494 was increased approximately twofold in the kidneys of mice treated with CsA compared to controls. Expression of miR-494 then decreases, and by 4 weeks after initiation of CsA treatment, expression is decreased relative to controls. The decrease in miR-494 expression observed at 4 weeks was dose dependent (Figure 2B), suggesting that the reduction in miR-494 expression is likely the result of the fibrosis and tubular loss resulting from CsA toxicity (Figure 1). We next examined whether an increase in miR-494 expression was a general feature of progressive renal injury by examining miR-494 expression following unilateral ureter obstruction (UUO). miR-494 was up-regulated to a similar degree in kidneys subject to UUO and CsA induced injury (Figure 2C). Dissection of CsA treated kidneys revealed that within the medulla, expression of miR-494 initially increased and then decreased over the 4-week time course analyzed (Figure 2D). CsA treatment also led to an increase in miR-494 expression within the renal cortex (Figure 2E).

CsA induced EMT is associated with upregulation of miR-494

Kidneys from mice treated with CsA exhibited significant fibrosis (Figure 1), leading us to hypothesize that miR-494 might play a role in EMT. To test this hypothesis, HK-2 cells (human tubular epithelial cell line) were treated with CsA. HK-2 cells treated with CsA lost their cobblestone appearance and adopted an elongated fibroblastoid appearance (Figure 3A). Treatment of HK-2 cells with CsA also led to an increase in expression of α-SMA (Figure 3A) and a reduction in the expression of the epithelial cell marker E-cadherin (Figure 3B and C). Alterations in morphology, increased expression of α-SMA, and a reduction in E-cadherin are consistent with induction of EMT by CsA (17). These changes were associated with a dose dependent increase in expression of miR-494 (Figure 3D). An increase

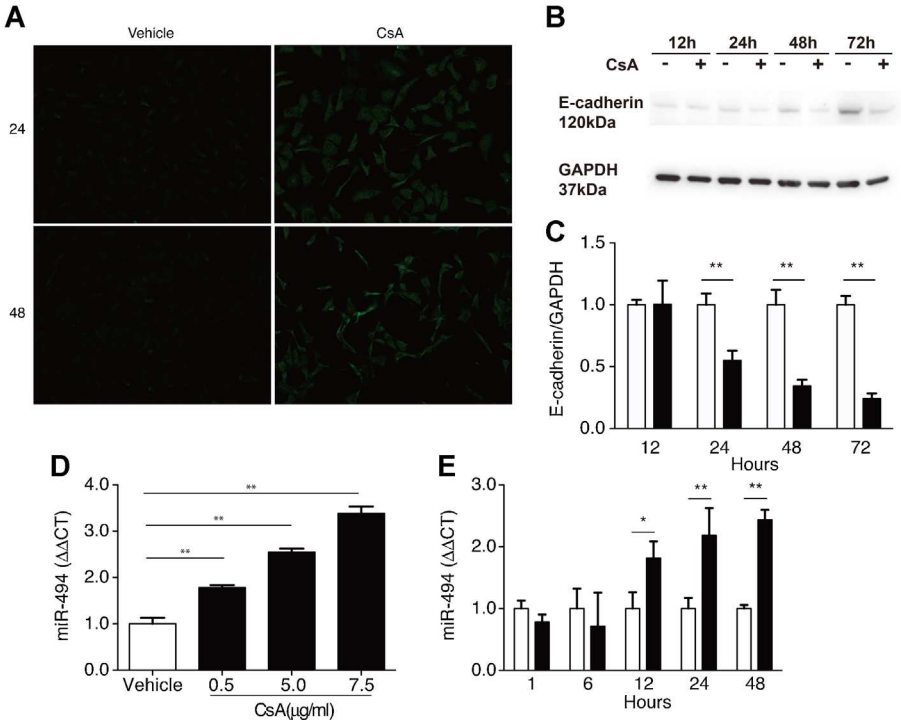

Figure 3: (A) Expression of α-SMA expression in HK-2 cells treated with 5 μg/mL CsA or vehicle (0.1% ethanol) for 24 h or 48 h detected by immunofluorescence (200×). Images were taken with identical exposure conditions. Photographs are representative of three independent experiments. (B) Expression of E-cadherin in HK-2 cells treated with vehicle or 5 μg/mL CsA for 12 h, 24 h, 48 h, and 72 h as assessed by Western blotting. GAPDH served as a loading control to normalize the data. (C) Quantification of E-cadherin expression in CsA (filled bars) and vehicle treated (open bars) HK-2 cells shown in panel B. Data were normalized to GAPDH. Data are representative of at least three independent experiments. Bars represent means ± SEM. (D and E) miR-494 expression in HK-2 cells treated with CsA. HK-2 cells were treated with vehicle or CsA (0.5 μg/mL, 5 μg/mL, or 7.5 μg/mL) for 72 h (D), or with vehicle (white bars) or 5 μg/mL CsA for 1 h, 6 h, 12 h, 24 h, or 48 h (filled bars, E). miR-494 expression levels were determined as above following normalization to U6 snRNA. Data are representative of at least three independent experiments.

in expression of miR-494 was observed as early as 12 h after CsA treatment and peaked at 48 h (Figure 3E).

Expression of miR-494 and PTEN exhibits an inverse relationship in tubular epithelial cells

To examine whether miR-494 plays a direct role in regulating CsA induced EMT, we sought to identify targets of miR-494 that might play a role in EMT. Bioinformatics analysis revealed that the 3′UTR of phosphatase and tensin homolog (*Pten*) is a potential target of miR-494. PTEN is a negative regulator of the PI3K/Akt pathway that plays a major role in EMT (18). Downregulation of PTEN leads to activation of the PI3K/AKT pathway thereby promoting EMT. The 3′UTR of *Pten* includes two potential miR-494 target sites that are conserved in humans and mice. We reasoned that upregulation of miR-494 resulting from CsA treatment might contribute to EMT by promoting the downregulation of PTEN. Treatment of HK-2 cells with CsA resulted in a reduction in PTEN levels over time (Figure 4A and B). The reduction in PTEN observed following CsA treatment was dose dependent (Figure 4A and C). In the kidney, reduction of PTEN (Figure 4D and E) over time followed changes in miR-494 expression (Figure 4D and E and Figure 2A). Thus, there is an inverse relationship between expression of miR-494 and PTEN levels in HK-2 cells treated with CsA and the kidneys of mice administered CsA.

miR-494 targets Pten *in tubular epithelial cells*

To examine whether miR-494 targets *Pten*, we transfected HK-2 cells with a reporter construct in which the 3′UTR of *Pten* was cloned downstream of luciferase (*Pten*-Luc). As a control, cells were transfected with an empty reporter construct. We then transfected the cells with a miR-494 mimic or scrambled control RNA. Transfection with the miR-494 mimic resulted in a reduction in luciferase activity in cells transfected with the 3′UTR *Pten* reporter (Figure 5A). We also transfected HK-2 cells with the miR-494 mimic or scrambled control RNA and examined the effect on PTEN levels. Transfection of HK-2 cells with a miR-494 mimic resulted in a reduction in endogenous PTEN levels (Figure 5B and C). We next examined whether reducing miR-494 expression with locked-nucleic acid (LNA) antagomirs altered PTEN levels in HK-2 cells following CsA treatment. Transfection of untreated HK-2 cells with miR-494 antagomirs resulted in a modest but significant increase in PTEN levels when compared to cells transfected with a scrambled antagomir control (Figure 5D and E). Knockdown of miR-494 in HK-2 cells treated with CsA prevented the reduction in PTEN levels (Figure 5D and F). When compared with control cultures treated with a

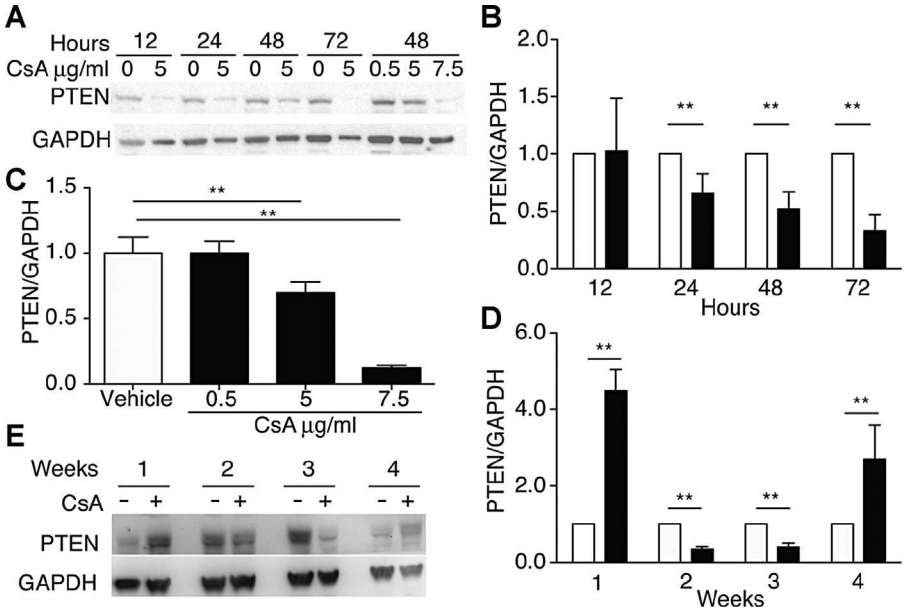

Figure 4: (A) Expression of PTEN in HK-2 cells treated with CsA over a 72-hour period as determined by Western blotting. GAPDH served as a loading control. (B) Expression of PTEN in HK-2 cells treated with 5 μg/mL CsA (filled bars) relative to HK-2 cells treated with vehicle over a 72-hour period as determined by Western blotting. Expression was first normalized to GAPDH before determining relative expression levels. (C) Expression of PTEN in HK-2 cells treated with various doses on CsA for 72 h relative to cells treated with vehicle quantitated as above. Data in B and C are representative of at least three independent experiments. Bars represent means ± SEM. (D) Relative expression levels of PTEN in the kidneys of mice treated with 30 mg/kg CsA (filled bars) at 1, 2, 3, or 4 weeks compared to controls receiving vehicle alone (open bars). PTEN expression was assessed by Western blotting following normalization to GAPDH (E). Data are representative of at least three independent experiments (n = 5 mice per group). Bars represent means ± SEM.

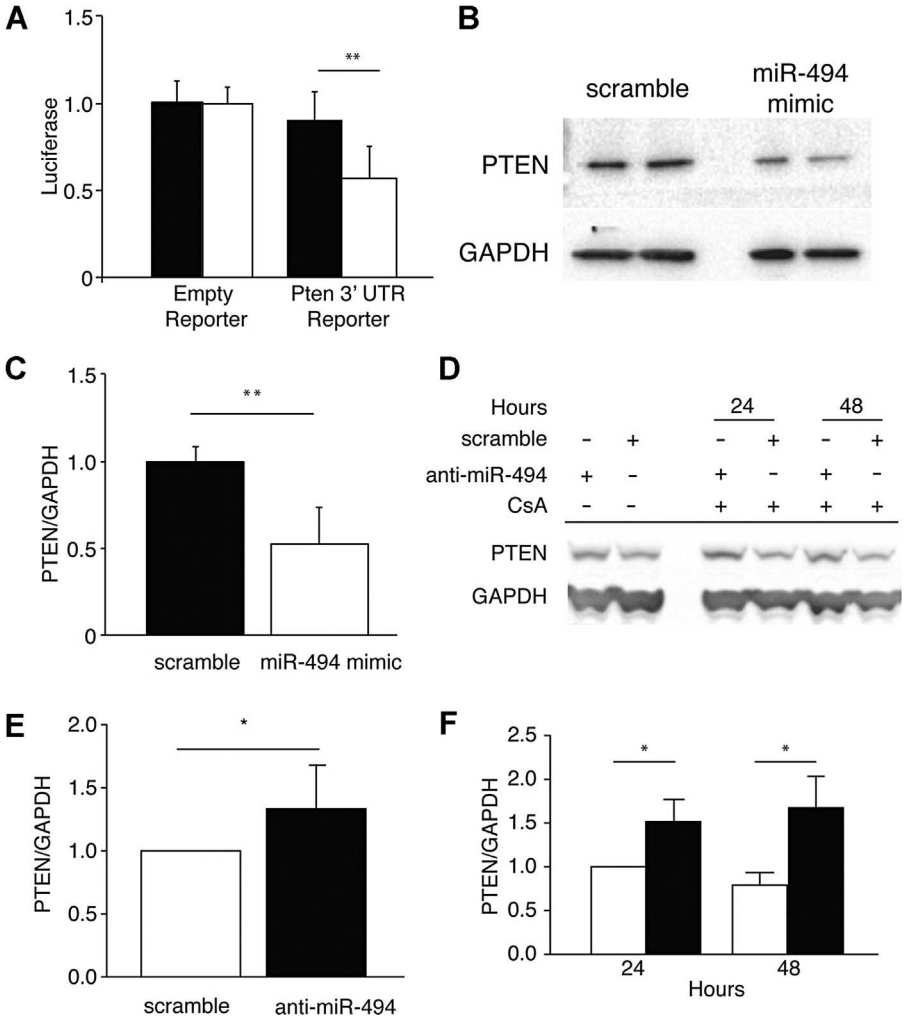

Figure 5: (A) HK-2 cells were transfected with *Pten*-Luc or a control luciferase reporter lacking the 3′UTR of *Pten*. The cells were then treated with a miR-494 or scrambled control miR mimic and luciferase activity assayed 48 h later. (B) Analysis of endogenous PTEN levels by Western blotting in HK-2 cells treated with a miR-494 or a scrambled control miR mimic. PTEN levels were analyzed in whole cell lysates 48 h after treatment with miR mimics. (C) Quantitation of relative PTEN levels in HK-2 cells treated with a miR-494 or a scrambled control miR mimic shown in panel B following normalization to GAPDH levels. Shown are relative expression levels. (D) HK-2 cells were transfected with a scrambled control or anti-miR-494 LNA antagomir for 24 h and then treated with 5 μg/mL CsA for 48 h. PTEN levels were then assessed by Western blot at 24 h and 48 h. GAPDH served as a loading control. (E) Quantitation of PTEN expression in HK-2 cells from data in panel D following knockdown of miR-494 in the absence of CsA relative to levels observed in cells treated with a scrambled control antagomir. (F) PTEN levels in HK-2 cells from data in panel D following knockdown of miR-494 in the presence of CsA. Filled bars represent relative expression levels in cells treated with the anti-miR-494 compared to expression in cells treated with a scrambled control antagomir. Data are representative of three independent experiments. Bars represent means ± SEM.

scrambled antagomir, knockdown of miR-494 in HK-2 cells treated with CsA resulted in an increase in PTEN (Figure 5D and F). Thus, knockdown of miR-494 reverses the down-regulation of PTEN induced by CsA in HK-2 cells. Together, these data indicate that miR-494 targets *Pten* and negatively regulates its expression.

miR-494 plays a central role in CsA-induced EMT

We next sought to determine whether EMT resulting from CsA treatment of HK-2 cells was due to targeting of *Pten* by miR-494. We therefore utilized a *Pten* expression construct that lacked the 3′UTR containing miR-494 target sequences found in full-length *Pten*. Transfection of HK-2 cells with this construct resulted in an increase in PTEN expression as expected (Figure 6A and B). We next examined whether expression of *Pten* lacking a miR-494 target sequence affected the ability of CsA to induce EMT. Following treatment with CsA, HK-2 cells transfected with a control vector began to express αSMA and underwent EMT as expected (Figure 6C). In contrast, induction of αSMA in

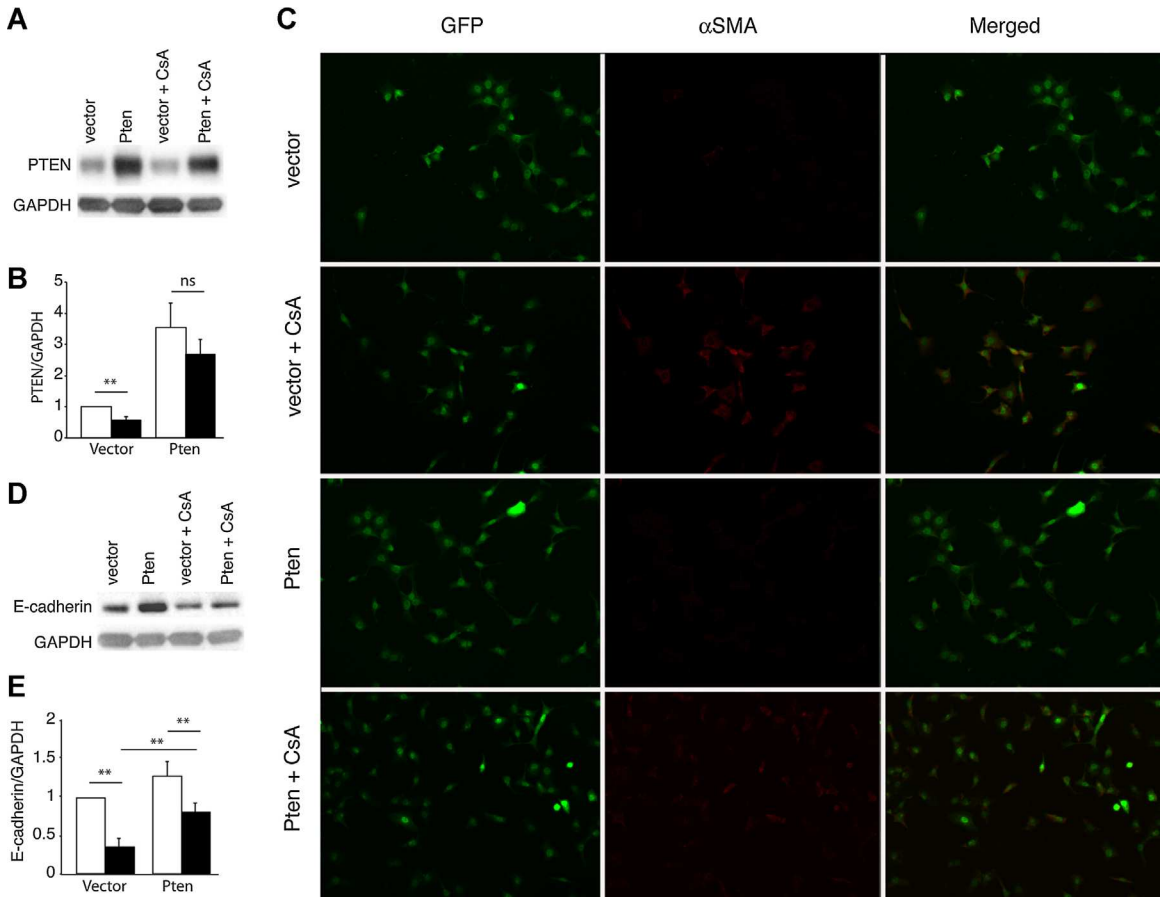

Figure 6: (A) HK-2 cells were transfected with an expression construct encoding *Pten* lacking a 3′UTR (Pten) or an empty vector (vector). The cells were then either left untreated or treated with CsA or vehicle. Shown are PTEN levels determined by Western blotting. (B) Quantitation of relative PTEN levels in panel A following normalization to GAPDH levels. (C) HK-2 cells transfected with a control or PTEN vector were treated with 5 μg/mL CsA or vehicle for 48 h and then stained with antibodies to GFP encoded in each vector and α-SMA. Images were then merged to assess α-SMA expression in transfected GFP+ cells. Expression (D) and quantitation (E) of E-cadherin in cells treated as described in panel A. Shown are representative data.

HK-2 cells transfected with the *Pten* construct lacking miR-494 targeting sequences was reduced when compared to cells transfected with control vector. Downregulation of E-cadherin after CsA treatment was also reduced in HK-2 cells transfected with the *Pten* construct compared to controls (Figure 6D and E). Thus expression of *Pten* lacking miR-494 target sequences prevented the ability of CsA to induce EMT. Therefore, preventing targeting of *Pten* by miR-494 was sufficient to prevent induction of EMT by CsA.

Knockdown of miR-494 prevents EMT

If upregulation of miR-494 as a result of CsA treatment promotes EMT through downregulation of PTEN, we reasoned that knockdown of miR-494 should prevent EMT. To test this hypothesis, HK-2 cells were transfected with miR-494 antagomirs and then treated with CsA for 24 h or 48 h. Control cultures were transfected with scrambled antagomirs and then treated with CsA. CsA treatment of HK-2 cells transfected with scrambled antagomirs resulted in reduced proliferation, morphologic changes resulting in an elongated shape, and an increase in expression of α-SMA (Figure 7A and B) as we observed previously. In contrast, HK-2 cells transfected with miR-494 antagomirs retained their cobblestone appearance, proliferated (Figure 7A) and did not increase expression of α-SMA (Figure 7B) when treated with CsA.

Discussion

Long-term use of CsA is associated with significant nephrotoxicity (1,19–21). Major components of CsA nephrotoxicity include tubular epithelial cell apoptosis and EMT (6–8), however it is unclear how these responses are regulated. Previous work from our laboratory has shown that miRs play a significant role in regulating renal

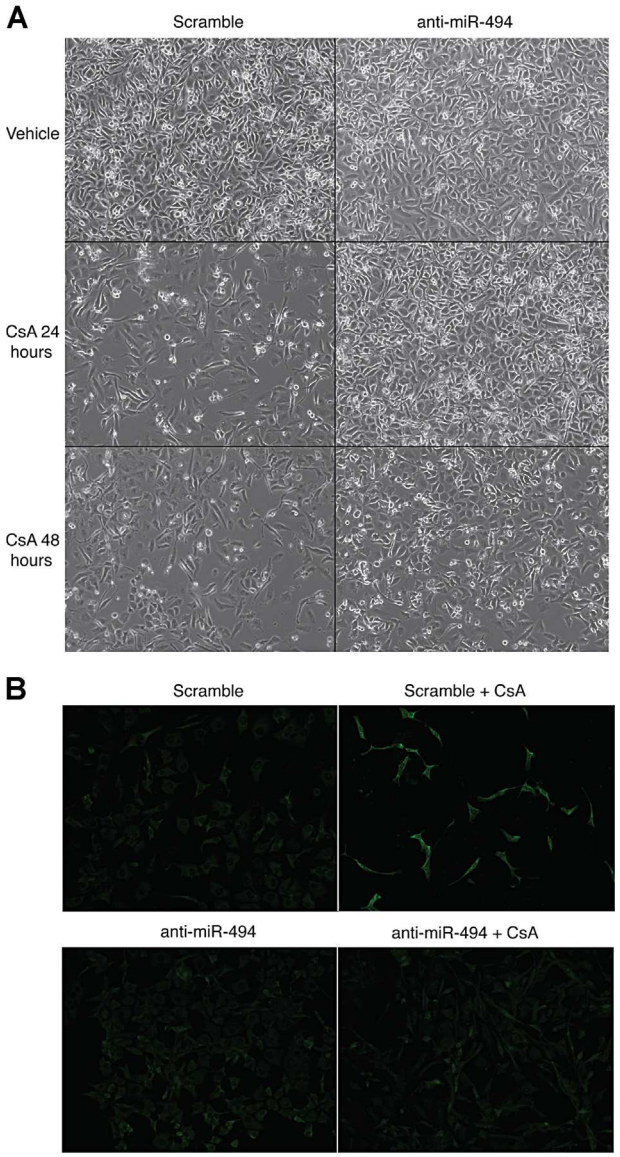

Figure 7: (A) HK-2 cells were transfected with scrambled or anti-miR-494 antagomirs for 24 h, and then treated with vehicle or 5 μg/mL CsA for 48 h. The cells were then analyzed by phase contrast microscopy at 24 h and 48 h (100 ×). (B) HK-2 cells grown on collagen-coated coverslips were transfected with scrambled or anti-miR-494 antagomirs for 24 h, and then treated with vehicle or 5 μg/mL CsA for 48 h. α-SMA expression was then analyzed by immunocytochemistry. Images were taken with identical exposure conditions (200×). Photographs are representative of three independent experiments.

injury (14,22). We therefore set out to examine whether miRs play a role in regulating renal injury resulting from CsA treatment by examining miRs that change as a result of CsA treatment. Our data suggest that CsA induced renal damage leads to an increase in the expression of miR-494. miR-494 was rapidly up-regulated after CsA treatment and returned to baseline over the following 2 weeks. At late time points after injury, we observed a dose dependent decrease in miR-494. Given that high doses on CsA lead to increased tissue injury, we suggest that the reduction in miR-494 expression observed at late time points is likely the result of the fibrosis and tubular loss resulting from CsA toxicity. We also observed that miR-494 expression increases following UUO while others have shown an increase in miR-494 after acute renal injury (18). We suggest that upregulation of miR-494 is a general feature of renal injury and that its upregulation participates in regulating injury.

CsA induced EMT was associated with an upregulation of miR-494. Insofar as negative regulation of the PI3K/AKT pathway by PTEN plays a role in preventing EMT (23) we reasoned that upregulation of miR-494 resulting from CsA treatment may contribute to EMT by promoting the down-regulation of PTEN. We observed an inverse relationship between expression of miR-494 and PTEN levels in the kidneys of mice administered CsA and in HK-2 cells treated with CsA. PTEN protein levels increased early after CsA treatment and then decreased following miR-494 upregulation. Subsequent increase in PTEN coincided with decrease in miR-494 levels at 4 weeks. The half-life of PTEN has been estimated to be as long as 48–72 h (24). Given that miRs regulate transcription, decreases in the level of proteins with a long half-life would be predicted to lag behind the upregulation of a miR that negatively regulates transcript levels. Indeed, we observe that expression of miR-494 and PTEN levels are inversely related in the kidney and that regulation of PTEN levels occurs in the predicted manner.

Reports in other systems have suggested that miR-494 can target *Pten* (25,26). Our data indicate that miR-494 directly targets *Pten* in tubular epithelial cells. Expression of a *Pten* construct lacking miR-494 targeting sequences prevented EMT following treatment of tubular epithelial cells with CsA. Knockdown of miR-494 revealed that the down-regulation of PTEN associated with CsA treatment was dependent on expression of miR-494 indicating a direct relationship. Together, these data show that miR-494 plays an important role in CsA nephrotoxicity and injury by promoting EMT through targeting of *Pten*.

Increased expression of miR-494 in the kidneys of mice was observed at 1 week after treatment, and then returned to baseline by week 2 and 3. This suggests that miR-494 appears to play a role in regulating responses that occur early after injury. One of the earliest responses to renal damage is proliferation (27), and it is well established that a general feature of EMT is excessive epithelial cell proliferation (28,29). Insofar as AKT signaling plays a critical role in regulating proliferation, we suggest that targeting *Pten*, a negative regulator of this pathway, through upregulation of miR-494 provides a mechanism by which proliferation of tubular epithelial cells is promoted, resulting in EMT. Interestingly, placing mice on a low salt diet was

also sufficient to result in an increase in miR-494 expression, even though a low salt diet was not sufficient to induce gross injury.

Given that knockdown of miR-494 was able to prevent EMT, we suggest that this miR represents a novel druggable target to prevent renal injury. Indeed, EMT results from a wide variety of chronic and acute injuries and developing novel strategies to prevent EMT would have significant clinical potential. Given that increases in miR-494 expression are associated with injury, while return to baseline is associated with resolution of injury, or repair, we suggest that changes in miR-494 expression may serve as a biomarker of renal injury. Given that miR-494 potentially targets many other genes in addition to *Pten*, it will be of interest to determine whether these genes are also targeted by miR-494 during renal injury and how their regulation through miR-494 contributes to renal injury.

Acknowledgments

This work was supported in part by a grant from the Roche Organ Transplantation Research Foundation to J.I., an American Heart Association Scientist Development Grant to J.B., and an American Society of Transplantation/Genentech Basic Science Fellowship Grant to J.Y and NIH grant R01AI83459-05. C.J.B. was also supported in part by NIH Institutional Training Grant T32AI070085.

Disclosure

The authors of this manuscript have no conflicts of interest to disclose as described by the *American Journal of Transplantation*.

References

1. Bennett WM, DeMattos A, Meyer MM, Andoh T, Barry JM. Chronic cyclosporine nephropathy: The Achilles' heel of immunosuppressive therapy. Kidney Int 1996; 50: 1089–1100.
2. Gipson DS, Trachtman H, Kaskel FJ, et al. Clinical trial of focal segmental glomerulosclerosis in children and young adults. Kidney Int 2011; 80: 868–878.
3. Fernandes IC, Torres T, Selores M. Maintenance treatment of psoriasis with cyclosporine a: Comparison between continuous and weekend therapy. J Am Acad Dermatol 2013; 68: 341–342.
4. Ojo AO, Held PJ, Port FK, et al. Chronic renal failure after transplantation of a nonrenal organ. N Engl J Med 2003; 349: 931–940.
5. Bobadilla NA, Gamba G. New insights into the pathophysiology of cyclosporine nephrotoxicity: A role of aldosterone. Am J Physiol Renal Physiol 2007; 293: F2–F9.
6. Justo P, Lorz C, Sanz A, Egido J, Ortiz A. Intracellular mechanisms of cyclosporin A-induced tubular cell apoptosis. J Am Soc Nephrol 2003; 14: 3072–3080.
7. Neria F, Castilla MA, Sanchez RF, et al. Inhibition of JAK2 protects renal endothelial and epithelial cells from oxidative stress and cyclosporin A toxicity. Kidney Int 2009; 75: 227–234.
8. Slattery C, Campbell E, McMorrow T, Ryan MP. Cyclosporine A-induced renal fibrosis: A role for epithelial-mesenchymal transition. Am J Pathol 2005; 167: 395–407.
9. McMorrow T, Gaffney MM, Slattery C, Campbell E, Ryan MP. Cyclosporine A induced epithelial-mesenchymal transition in human renal proximal tubular epithelial cells. Nephrol Dial Transplant 2005; 20: 2215–2225.
10. Trionfini P, Benigni A, Remuzzi G. MicroRNAs in kidney physiology and disease. Nat Rev Nephrol 2014; 14: 1046–1060.
11. Andoh TF, Lam TT, Lindsley J, Alpers CE, Benneti WM. Enhancement of chronic cyclosporine nephrotoxicity by sodium depletion in an experimental mouse model. Nephrology 1997; 3: 471–478.
12. Yang CW, Faulkner GR, Wahba IM, et al. Expression of apoptosis-related genes in chronic cyclosporine nephrotoxicity in mice. Am J Transplant 2002; 2: 391–399.
13. Chevalier RL, Forbes MS, Thornhill BA. Ureteral obstruction as a model of renal interstitial fibrosis and obstructive nephropathy. Kidney Int 2009; 75: 1145–1152.
14. Godwin JG, Ge X, Stephan K, Jurisch A, Tullius SG, Iacomini J. Identification of a microRNA Signature of renal ischemia reperfusion injury. Proc Natl Acad Sci USA 2010; 107: 14339–14344.
15. Carlisle RE, Heffernan A, Brimble E, et al. TDAG51 mediates epithelial-to-mesenchymal transition in human proximal tubular epithelium. Am J Physiol Renal Physiol 2012; 303: F467–F481.
16. Djamali A, Reese S, Hafez O, et al. Nox2 is a mediator of chronic CsA nephrotoxicity. Am J Transplant 2012; 12: 1997–2007.
17. Kriz W, Kaissling B, Le Hir M. Epithelial-mesenchymal transition (EMT) in kidney fibrosis: Fact or fantasy. J Clin Invest 2011; 121: 468–474.
18. Lan YF, Chen HH, Lai PF, et al. MicroRNA-494 reduces ATF3 expression and promotes AKI. J Am Soc Nephrol 2012; 23: 2012–2023.
19. Chapman JR. Chronic calcineurin inhibitor nephrotoxicity-lest we forget. Am J Transplant 2011; 11: 693–697.
20. de Mattos AM, Olyaei AJ, Bennett WM. Nephrotoxicity of immunosuppressive drugs: Long-term consequences and challenges for the future. Am J Kidney Dis 2000; 35: 333–346.
21. Yang CW, Ahn HJ, Kim WY, et al. Influence of the renin-angiotensin system on epidermal growth factor expression in normal and cyclosporine-treated rat kidney. Kidney Int 2001; 60: 847–857.
22. Shapiro MD, Bagley J, Latz J, et al. MicroRNA expression data reveals a signature of kidney damage following ischemia reperfusion injury. PLoS ONE 2011; 6: e23011.
23. Carew RM, Wang B, Kantharidis P. The role of EMT in renal fibrosis. Cell Tissue Res 2012; 347: 103–116.
24. Wu X, Hepner K, Castelino-Prabhu S, et al. Evidence for regulation of the PTEN Tumor suppressor by a membrane-localized multi-PDZ domain containing scaffold protein MAGI-2. Proc Natl Acad Sci USA 2000; 97: 4233–4238.
25. Lorenzen JM, Batkai S, Thum T. Regulation of cardiac and renal ischemia-reperfusion injury by microRNAs. Free Radic Biol Med 2013; 64: 78–84.
26. Wang X, Zhang X, Ren XP, et al. MicroRNA-494 targeting both proapoptotic and antiapoptotic proteins protects against ischemia/reperfusion-induced cardiac injury. Circulation 2010; 122: 1308–1318.
27. Yang L, Besschetnova TY, Brooks CR, Shah JV, Bonventre JV. Epithelial cell cycle arrest in G2/M mediates kidney fibrosis after injury. Nat Med 2010; 16: 535–543, 531p following.
28. Strutz F, Muller GA. Transdifferentiation comes of age. Nephrol Dial Transplant 2000; 15: 1729–1731.

29. Schramek H, Feifel E, Healy E, Pollack V. COnstitutively active mutant of the mitogen-activated protein kinase kinase MEK1 Induces epithelial dedifferentiation and growth inhibition in madin-darby canine kidney-C7 cells. J Biol Chem 1997; 272: 11426–11433.

Supporting Information

Additional Supporting Information may be found in the online version of this article.

Figure S1: Quantitation of arteriolopathy (A) and tubular injury (B) in tissue sections from kidneys of mice treated with CsA or vehicle. (C) Serum creatinine levels in mice treated with CsA or vehicle. Quantitation of (E) E-cadherin and (F) α-SMA expression in lysates of kidneys from mice treated with CsA and vehicle controls by Western blot. Data were normalized to GAPDH. Data are representative of at least three independent experiments. Bars represent means $\pm$ SEM.